ERS Radar Interferometry: Absence of Recent Surface Deformation Near the Aswan Dam

Andrew K. Gabriel, Richard M. Goldstein, Ronald G. Blom*
Mail Stop 300-233
Jet Propulsion Laboratory
4800 Oak Grove Dr.
Pasadena, California 91109
(*RGB corresponding author)

Abstract

Seismic activity in the region of the Aswan Dam in southeastern Egypt has likely been induced by mass loading associated with initial filling and recent high water levels in Lake Nasser (Awad and Mizoue, 1995; Vyskocil, et. al., 1991). Measurement of surface deformation (strain) resulting from any of several sources, such as seismic events, landslides, or mass loading are of potential interest to reservoir operations. In this paper the potential utility of synthetic aperture radar interferometry, or InSAR, as an additional tool for regional monitoring of large reservoirs is demonstrated. Data from the ERS-1 (European Radar Satellite) and ERS-2 satellites taken in the period 5/96-4/98 was used to search for any surface changes within about 100km of the dam. No deformation along the line of sight was observed in excess of a calculated upper bound of 5 mm (derived from phase noise in the image) over the period of observation. The experiment demonstrates the utility of a satellite specifically designed for InSAR observations which could provide superior, ongoing measurements of surface deformations relevant to reservoir management and dam safety.

Introduction and Review

In all types of synthetic aperture radar interferometry, multiple radar images of a given scene are generated, and the phases associated with corresponding resolution elements are differenced. In the simplest configurations, two radar images are used to generate surface topography (Zebker and Goldstein, 1986) with corrections for nonparallel orbits (Gabriel and Goldstein, 1988) or to measure surface ocean currents (Ainsworth, et. al., 1995). The newer technique of double difference interferometry (DDI) uses an additional third image to remove the same topography, revealing any deformation of the surface which occurred

over the time period of the observations to very high accuracy, often approaching mm scale (Gabriel, et al., 1989). This latter method has been used with great success to measure deformation from earthquakes (Zebker, et. al., 1994; Peltzer, et. al., 1994, 1996, 1998, 1999, Peltzer and Rosen, 1995), volcanic inflation (Lanari, et. al., 1998, Rosen, et al., 1996), oilfield subsidence (Fielding, et al., 1998) subsidence due to ground water depletion (Peltzer and Rogez, 1997), and to measure glacier motion (Goldstein, et al., 1993).

Double Difference Interferometry

Formation of Interferograms: General Description

Following the derivation in Gabriel and Goldstein (1988), double difference interferometry begins with three suitable complex (amplitude and phase) sets of radar data of a given scene - radar echoes that have been compressed and focused in the along-track (azimuth) and cross-track (range) directions. The basic radar data requirements are spatial coverage of the scene of interest, temporal coverage spanning the event of interest, and the maintenance of phase coherence across the image pairs. This last constraint, derived from the physical phenomenon of speckle decorrelation, places strict upper bounds on the satellite orbit separation ("baselines") and mandates that any significant changes to the surface, including the event of interest, occur on scales larger than the areal resolution of the radar[1]. It also invokes the more relaxed criterion that the scene be free of extensive areas where topography alone causes decorrelation[2] (Zebker et al., 1994). Areas of high relief and rugged topography can have this problem.

Next, an estimate of the three baselines corresponding to each pair of the three images is made from orbit tracking data. Using (usually) the pairs of images with the two shortest

---

[1] For example, an elevation change from an earthquake can be measured because the surface scattering characteristics of individual resolution cells do not change (except possibly near fault rupture). Conversely, a landslide will completely change the speckle signatures by disrupting the surface within the cells, destroying the phase information needed for interference. Minor motion before a landslide might however be measured.

[2] Phase variation accompanying altitude changes may exceed the Nyquist rate in steep terrain. Also in the phenomenon usually termed "layover", topography that serendipitously matches the spherical wavefront of the radar has more stringent baseline

baselines, the two 'different' images are resampled to overlay the 'common' image. This compensates for shearing or other distortions which occur from nonparallel orbits (e.g., baselines that vary in azimuth). Then two conventional or "single difference" interferograms (SDI's) are constructed by calculating, for each pair, the product of one image with the complex conjugate of the other. The phase of each SDI is then unwrapped by any of several standard techniques (Ghiglia and Pritt, 1998), a step that is often quite difficult and excludes areas with surface decorrelation and frequently areas with unfavorable topography as well.

Finally, the phase in each SDI is scaled by its own fixed baseline and one SDI is multiplied by the complex conjugate of the other, yielding a "double difference" interferogram (DDI). At this stage, if the three orbits were perfectly parallel (nonvarying baselines) and coplanar, the global phase would be constant in the DDI except where deformation occurred; that is, the scaled topographic phases in the two SDI's would cancel exactly. The physical deformation along the line of sight to any given cell could then be calculated[3], yielding a deformation map showing the projection of surface deformation along the line of sight.

Baseline Error

In practice, there is almost always varying phase in such a DDI, either from areas of decorrelation, which yield noiselike phases or from the geometric errors of noncoplanar[4] or nonparallel orbits, which produce moderately complex regional fringes (e.g. non-noisy phases) even over a completely flat scene. Furthermore, when the scene is not flat, for almost all azimuths, the small *de facto* baseline errors result in DDI fringes that, while dominated by geometric effects, have a weak but visible topographic component (Gabriel and Goldstein, 1988). These errors can mask the desired deformation phases, and must be corrected. In mathematical terms, the geometric errors require equation 4 of Gabriel, et al., (1989) to have quadratic terms in both azimuth and range;

---

requirements than flat areas in the scene. In either case, the result can be localized areas of decorrelation associated with topography.

[3] There is usually ambiguity as to whether the motion occurred in the period of time spanned by the first or the second SDI.

$$\Phi = \phi_{1,2}/p - \phi_{2,3}/q + c_1 + c_2 x^2 + c_3 y^2$$

Phase correction can be accomplished either by deducing the actual varying baselines from the scenes (e.g. Zebker, et al., 1994, Gabriel and Goldstein, 1988) and recalculating the phases in azimuth and range, or by the more empirical approach of removing the lowest spatial frequencies on the surmise that they originate in orbit geometry. The former approach is rigorous but more difficult; the latter posits an assumption but is easier, and was used below. This choice precludes detection of very long spatial wavelength (many tens of kilometers) deformations.

Error Correction: Ellipse Picture

In the formulation of Gabriel, et al, (1989) for scenes 1,2 and 3, where p and q are the SDI baselines, the normalized phase $\phi_a=\phi_{1,2}/p$ of one SDI plotted against the other, $\phi_b=\phi_{2,3}/q$, forms a segment of the locus of an ellipse. Deformations appear as a local, ordered deviation from the ellipse, and phases corresponding to decorrelated pixels appear as randomly scattered points. The shape of the ellipse changes with azimuth (y) if p or q so changes. Thus in the absence of deformations or decorrelation, all the SDI phases lie on a surface $E=\phi_a(\phi_b,y)$, the intersection of which with any ϕ_a,ϕ_b plane is an ellipse segment.

However, the real data, scaled to fixed, implicitly coplanar baselines p and q do not produce E but a distortion E' that expresses the geometric errors as well. These errors were removed empirically by constructing a multivariable least squares fit to E':[5]

$$E'' = \text{fit to } \{\phi_b, \phi_b^2, y, y^2, y\phi_b, \text{constant}\} \qquad (1)$$

---

[4] The angle between the two baselines in the plane perpendicular to the orbits is zero for coplanar orbits.

The low (n=2) order of the polynomial meant phases which varied slowly – assumptively those originating in the geometry of the ellipses and geometric errors - would count most heavily in determining the coefficients. The phase resulting from any deformation in the 'a' interval was then calculated as the distance in the ϕ_a direction from any data point to the constructed surface E''; similar comments apply to the 'b' interval and the ϕ_b direction.[3] Finally, the residual phase variance in undisturbed areas of the scene from all sources was estimated as the perpendicular distance in the ϕ_a,ϕ_b plane to E'', which, as noted in Gabriel, et. al., (1989), is some intermediate value.

The Aswan Dam and Lake Nasser

The filling of Lake Nasser pursuant to the construction of the Aswan dam was accompanied by seismic events evidently caused by the additional water mass (Awad and Mizoue, 1995). In particular the Kalabsha fault, ~50km south of the dam itself, was reported to have moved somewhat in tandem with the backfilling (Vyskocil, et al., 1991), including the November 14, 1981 Mw 5.3 event. More recent reports describe seismic activity apparently correlated with very high water levels spanning the last few years (Awad and Mizoue, 1995; Kebeasy and Gharib, 1991). Any significant surface deformation during the observation period might be visible with InSAR methods applied to ERS data. For example, aseismic deformation related to pore fluid migration has been mapped using InSAR (Peltzer, et al., 1996).

---

[5] Since the a,b ordering is arbitrary, the curve fitting can be done in two equivalent ways. It was assumed that the deformed areas of the scene were small and did not significantly affect the calculation of E'; also decorrelated areas were not used in the fit.

Aswan Site Data

There were a total of four orbits during which ERS 1 and 2 observed the area around the reservoir, three of which had baselines short enough to be suitable for interferometry.

Number	Date	Orbit	Satellite	Frame	% missing lines
1	5/23/96	25388	ERS-1	3123	0
2	8/22/97	12228	ERS-2	3123	11.4
3	4/24/98	15735	ERS-2	3123	5.5

The 1-2 baseline was approximately –312m; the 2-3 baseline approximately +81m.

Water Level Records

Figure 1 below shows the water level in Lake Nasser for the period 1994 – 1998 which encompasses the observation period (Dr. T. Ramadan, personal communication.) The increase in water level over time is apparent, particularly after 1994. The annual decrease in level is due to water release for irrigation. The three vertical lines indicate the times of the ERS radar data acquisitions used for interferometric analysis and listed in the table above.

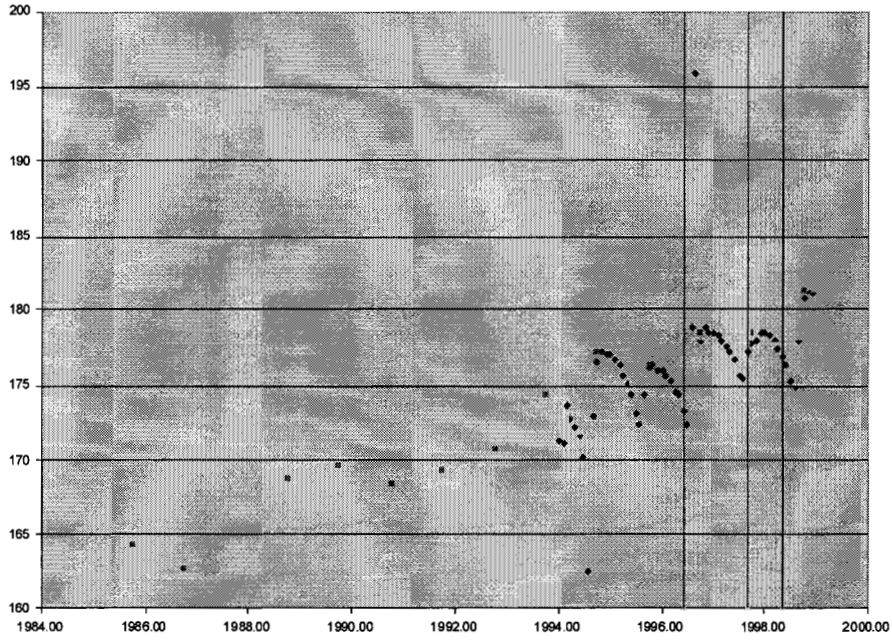

Figure 1. Water Level of Lake Nasser 1994-8 measured at the Aswan High Dam (meters above sea level). The vertical lines are the dates of ERS observations. The two anomalous data points are probably errors.

The second and third observations occurred at approximately the same water levels. However, the level of the lake was clearly lower at the time of the first pass.

Aswan Interferogram

The DDI corresponding to the data in Table 1 is presented in Fig. 2. It was processed in the manner described above, including the empirical baseline corrections leading to E".

(Figure 2 here) - AT END OF MS.

Figure 2. Deformation interferogram of the northern part of Lake Nasser. The Aswan dam is the small curved structure visible where the lake narrows. Deformation (DDI phase) is

encoded as color; regions of uniform color are unchanged. The slow gradations in color are correlated with topography, implying imperfect estimation of the baselines rather than deformation. The higher frequency changes are probably atmospheric in origin, as they do not correlate in any obvious way with surface features.

Completely absent in Figure 2 are fringes that originate in any obvious fashion from surface deformation near the reservoir, the dam, or Kalabsha Fault, which runs under the largest bay in the lake, just off the south end of the image. It therefore appears that no surface deformation larger than the phase errors, or about 5 mm along the line of sight, occurred during the observation period. Although no deformation was observed, the ability to construct useful interferograms indicates that the InSAR methodology has potential for observation of the land around large bodies of water and any associated structures such as dams. Sakr, et. al., (1999) began GPS surveying of the Lake Nasser region in 1997. It is worth noting that they report a GPS observation indicating 10mm of southwestward deformation at a point south of the Kalabsha Bay, which is unfortunately a few km south of our data. If real, this particular GPS measurement is probably a local effect as we would expect to see some deformation at the south end of our interferogram.

Error Sources; Upper Bound for Motion

Because the ERS satellites are not designed for routine InSAR observations, the timing of the observations was not optimal. Deformation related to mass loading is expected to lag the load; however, it is very unlikely that this would occur at just the right rate to account for the zero result. Alternatively, the response may have been so slow that no detectable deformation occurred during the 23 month observation time; this possibility is beyond the scope of the current work. Finally, the quadratic curve-fitting of Equation 1 could remove, at least partially, any low spatial frequency phases associated with gradual deformations (approximate quadratic curves) across the entire image (i.e. deformation with a 60km wavelength would be removed). This also seems unlikely to produce a zero result, given

the complex shape of both the lake and any resulting loading. Note that higher spatial frequency deformations would of course be detectable.

The slight phase changes correlated with topography observed in Figure 2 indicate that E'', unsurprisingly, still contains small global geometric errors. Atmospheric moisture (Goldstein, 1995) is an additional likely source of error, along with the usual sources of phase noise originating in radar hardware. The nominal observed RMS phase error, computed (above) as the perpendicular distance to E'' is approximately 5 mm, and constitutes an upper bound for deformation along the line of sight during the observation period.

Summary and Conclusion

Following a brief description of interferometric radar processing and error analysis, radar interferograms for the region surrounding the Aswan dam and Lake Nasser were presented and analyzed. Although high water levels and seismic events in the region are reported the same period of time, no significant deformation was observed. An upper bound for any line of sight deformation was derived from an analysis of the phase noise in the image and found to represent about 5 mm at the surface. The elapsed time from the load increase to the observation time or the observation period may have been too short for any observable deformation to occur; alternatively, it is possible that the load was inadequate to cause a detectable deformation. The ability to monitor large regions such as Lake Nasser and structures such as the Aswan Dam remotely with radar interferometry is a potentially significant complement to traditional surveying methods such as GPS. If a dedicated InSAR satellite were built, such observations could become routine within a few years.

Acknowledgements

The authors gratefully acknowledge the support of Dr. Talaat Ramadan, Egyptian National Authority for Remote Sensing and Space Sciences, who supplied the water level data. We

thank Eric Fielding and Erik Ivins for useful discussion and comment. We also wish to acknowledge support of the LightSAR project. Work performed at the Jet Propulsion Laboratory of the California Institute of Technology under contract with the National Aeronautics and Space Administration.

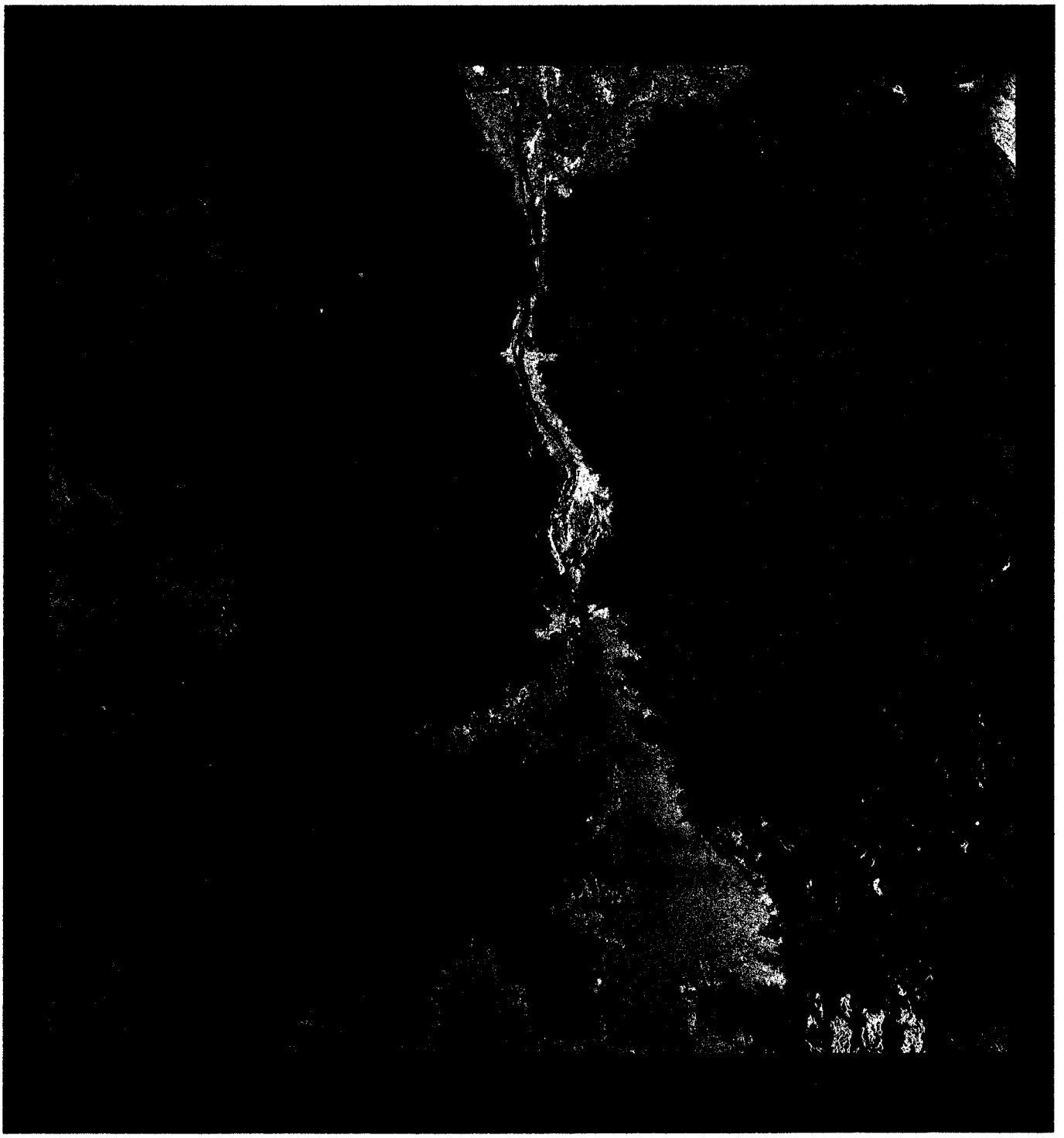

Fig. 2. Original in color.

References cited:

Awad, M., and M. Mizoue., 1995, Earthquake activity in the Aswan Region, Egypt: Pure and Applied Geophysics (Pageoph), v. 145, pp. 69-86.

Ainsworth T. L., et al., 1995, INSAR Imagery Of Surface Currents, Wave-Fields, and Fronts: IEEE Trans. Geosci. Remote Sensing, vol. 33, no. 5, pp. 1117-1123.

Fielding, E. J., R. G. Blom, and R. M. Goldstein, 1998, Rapid Subsidence Over Oil Fields Measured By SAR Interferometry: Geophysical Research Letters, v. 25, p. 3215-3218.

Gabriel, A. K. and R. M. Goldstein, 1988, Crossed Orbit Interferometry: Theory and Experimental Results From SIR-B: Int. J. Remote Sensing, vol. 9, no. 8, pp. 857-872.

Gabriel, A. K., R. M. Goldstein, and H. A. Zebker, 1989, Mapping Small Elevation Changes Over Large Areas: Differential Radar Interferometry: Jour. Geophys. Res. vol. 94, no. B7, pp. 9183-9191.

Ghiglia, Dennis C., and Mark D. Pritt , 1998. Two Dimensional Phase Unwrapping, John Wiley.

Goldstein, R., 1995, Atmospheric limitations to repeat-track radar interferometry: Geophysical Research Letters, vol. 22, pp. 2517-2520.

Goldstein, R. M., T. P. Barnett, and H. A. Zebker, 1989, Remote Sensing of Ocean Currents: Science, vol. 246, pp.1282-1285.

Goldstein, R. M., H. Engelhardt, B. Kamb, and R. M. Frolich, 1993, Satellite Radar Interferometry for Monitoring Ice-Sheet Motion: Application to an Antarctic Ice Stream: Science, vol. 262, p. 1525.

Kebeasy, R.M. and A.A. Gharib, 1991, Active Fault And Water Loading Are Important Factors In Triggering Earthquake Activity Around Aswan Lake: Journal Of Geodynamics v14 (1-4) : pp73-85.

Lanari, R., P. Lundgren, and E. Sansosti., 1998, Dynamic deformation of Etna volcano observed by satellite radar interferometry: Geophysical Research Letters. v. 25, p. 1541-1544.

Peltzer G., Hudnut K. W., Feigl K. L., 1994, Analysis of Coseismic Surface Displacement Gradients Using Radar Interferometry - New Insights Into the Landers Earthquake: Journal Geophys. Research 99, 21971-21981.

Peltzer G., Rosen P., 1995, Surface Displacements of the 17 May 1993 Eureka Valley, California, Earthquake Observed By SAR Interferometry: Science 268: (5215) 1333-1336.

Peltzer G, Rosen P, Rogez F, et al., 1996, Postseismic rebound in fault step-overs caused by pore fluid flow: Science 273: (5279) 1202-1204 .

Peltzer, G., and F. Rogez, 1997, Proc. 3rd ERS Symp. On Space at The Service of Our Environment, Florence, Italy, 17-21, ESA SP-414, 3 Vols., May 1997.

Peltzer G, Rosen P, Rogez F, et al., 1998, Poroelastic rebound along the Landers 1992 earthquake surface rupture: Jour. Geophys. Res 103, 30131-30145 DEC 10 1998

Peltzer G., Crampe F., King G., 1999, Evidence of nonlinear elasticity of the crust from the Mw7.6 Manyi (Tibet) earthquake: Science 286: (5438) 272-276.

Dr. Talaat Ramadan, 1999, Egyptian National Authority for Remote Sensing and Space Sciences; private communication.

Rosen, P. A., S. Hensley, H. A. Zebker, F. H. Webb, and E. J. Fielding, 1996, Surface Deformation and Coherence Measurements of Kilauea Volcano, Hawaii, From SIR-C Radar Interferometry: Jour. Geophysical Research, vol. 101, no. E10, pp. 23,109 - 23,126.

Sakr. K., H. Khalil, A. Tealeb, S. Mahmoud, and A. S. Mohamed, 1999, GPS measurements Around Nasser Lake for Monitoring Crustal Deformation Aswan Egypt: Program and Abstracts, International Symposium on GPS., Oct. 18-22, Tsukuba Japan, Abstract 06-08.

Vyskocil, P. A. Tealeb, R. Kebeasy, S. Mahmoud, 1991, Present State Of Geodynamic Properties of Kalabsha Area, Northwest of Aswan Lake, Egypt: Journal of Geodynamics v14 (1-4) : pp221-247.

Zebker, H. A., and R. M. Goldstein, 1986, Topographic Mapping From Interferometric Synthetic Aperture Radar Observations: Jour. Geophys. Res., vol. 91, no. B5, pp. 4,993 – 4,999.

Zebker, H. A., P. A. Rosen, R. M. Goldstein, A. Gabriel, and C. Werner, 1994, On The Derivation Of Coseismic Displacement Fields Using Differential Radar Interferometry: The Landers Earthquake: Jour of Geophysical Research, vol.99, no. B10, pp. 19,617 - 19,634.